Journal of Applied Pharmaceutical Science Vol. 12(08), pp 048-056, August, 2022
Available online at http://www.japsonline.com
DOI: 10.7324/JAPS.2022.120806
ISSN 2231-3354

Application of the central composite design approach for optimization of the nanosilver formula using a natural bioreductor from *Camellia sinensis* L. extract

Rini Dwiastuti[1], Phingkan Alamanda Suhendra[1], Sri Hartati Yuliani[1], Florentinus Dika Octa Riswanto[2*]

[1]Division of Pharmaceutics and Pharmaceutical Technology, Faculty of Pharmacy, Universitas Sanata Dharma, Yogyakarta 55282 Indonesia
[2]Division of Pharmaceutical Analysis and Medicinal Chemistry, Faculty of Pharmacy, Universitas Sanata Dharma, Yogyakarta 55282 Indonesia

ARTICLE INFO

Received on: 12/10/2021
Accepted on: 21/06/2022
Available Online: 04/08/2022

Key words:
Bioreductor, *Camellia sinensis* L., optimization, response surface methodology.

ABSTRACT

In recent years, the interest in applying the nanosilver technology in the medical field has increased due to its benefit for microbial inactivation. A natural bioreductor was chosen and developed in the nanosilver formulation to minimize the toxicity effects. The content of rutin makes it possible to develop an alternative bioreductor agent using black tea (*Camellia sinensis* L.) leaves extract. The aim of this research was to optimize the nanosilver formula consisting of black tea leaf extract and $AgNO_3$ with the employment of central composite design. The visible absorption wavelength and transmittance percentage were observed as dependent variables. The presence of rutin in the black tea leaves extract was proved using the thin-layer chromatography (TLC) technique. It was found that the extract concentration of 2.131% (m/v) and the $AgNO_3$ concentration of 1.379 mM were stated as the computational recommendation resulting from the predictive model with a composite desirability value at 0.998. These optimum conditions were applied in the synthesis of six nanosilver formula replications and resulted in the percentage of a prediction relative error of absorption wavelength and transmittance which were in the ranges of 1.18%–9.18% and 2.72%–8.64%, respectively. The Relative Standard Deviation (RSD) values of absorption wavelength and transmittance were 2.81% and 2.21%, respectively. The Z-average of the nanosilver particles was 124.8 nm.

INTRODUCTION

Nanosilver particles, silver particles with the size of 1–100 nm, have been widely studied due to their antimicrobial activities. Nanosilver particles were reported to have a broad antibacterial effect on both Gram-negative and Gram-positive bacterial as well as antibiotic-resistant bacterial strains (Ge *et al*., 2014). The nanosilver technology can be applied in the manufacturing process of sanitary napkins, cotton fibers, antiseptic sprays, and antimicrobial coatings for the sterilization of medical devices (Deshmukh *et al*., 2019; Ge *et al*., 2014; Ravindra *et al*., 2010; Sankar *et al*., 2016). Other publications reported that nanosilver particles were successfully synthesized to formulate antibacterial peel-off facial masks and produce other antibacterial agents (Badnore *et al*., 2019; Sastry *et al*., 2019; Vishwasrao *et al*., 2019). The size of nanosilver particles was stated as an important consideration since the decreasing of the size might affect the increasing of antibacterial activity of the material (Dong *et al*., 2019). Nanosilver particles can be synthesized in three different ways: chemical, physical, and biological methods (Ge *et al*., 2014). The chemical reduction method was commonly applied since it was reported as an easy, fast, and inexpensive method (Pulit *et al*., 2015). In the synthesis of nanosilver particles by the chemical reduction method, the usage of reducing agents may result in toxic effects and cause several environmental issues to remain (Demchenko *et al*., 2020; Li *et al*., 2011). Hence, the usage of natural reducing agents obtained from plants can be applied in the nanoparticles technology in order to decrease its toxicity

**Corresponding Author*
Florentinus Dika Octa Riswanto, Division of Pharmaceutical Analysis and Medicinal Chemistry, Faculty of Pharmacy, Universitas Sanata Dharma, Yogyakarta 55282 Indonesia
E-mail: dikaocta @ usd.ac.id

and support the development of green chemistry (Li *et al*., 2011; Rengga *et al*., 2017). Bioreductors from plants can be developed since their secondary metabolites such as flavonoids, saponins, tannins, and terpenoids (Handayani *et al*., 2020; Maarebia *et al*., 2019) were reported to provide antioxidant activity (Maarebia *et al*., 2019). In the previous study, some extracts from natural products were reported to be involved in nanoparticle synthesis such as *Andrographis paniculata* Ness. leaves (Wendri *et al*., 2017), *Averrhoa bilimbi* L. leaves (Aryantini *et al*., 2017), and *Tristaniopsis merguensis* leaves (Fabiani *et al*., 2019).

Compounds of terpenoids, phenolics, flavonoids, tannins, saponins, and alkaloids were classified as a class of the polyphenol bioreducing agents (Handayani *et al*., 2020; Maarebia *et al*., 2019; Rengga *et al*., 2017). Polyphenol compounds with antioxidant activity were reported to have the dominant amount in the tea extract (Tong *et al*., 2019; Turkmen *et al*., 2007). Jiang *et al*. (2015) reported that the black tea extract contained the most polyphenols content compared to other types of tea, namely, green tea and oolong tea (Tariq *et al*., 2010).

Black tea leaves contain several polyphenol compounds such as catechins, tannins, rutin, theaflavins, and thearubigin (Anesini *et al*., 2008; Latos-Brozio and Masek, 2019; Tong *et al*., 2019). It is important to select an appropriate water-soluble bioreductor in order to result in an optimized reaction with the $AgNO_3$ solution (Christania *et al*., 2020). The most abundant polyphenol compound in the aqueous extract of black tea leaves was rutin (Tong *et al*., 2019). Rutin, a glycoside of the flavonoid quercetin with a molecular formula of $C_{27}H_{30}O_{16}$, is soluble in water with a solubility of 130 mg/l (Aizawa *et al*., 2018; Enogieru *et al*., 2018; PubChem, 2020). According to the research conducted by Tong *et al*. (2019), each gram of black tea leaf powder (*Camellia sinensis* L.) contains 24.8 mg of rutin equivalent. Therefore, rutin can be extracted from black tea leaves using the infundation method to produce an infusion extract.

In the synthesis of nanosilver particles, the concentrations of precursors and bioreductors need to be considered. When the concentration of the precursor ($AgNO_3$) that was added is relatively high, the resulting nanosilver particles will be larger (Kupiec *et al*., 2011). On the other hand, when the concentration of the bioreductor increases, the resulting nanosilver particle size will decrease (Khalil *et al*., 2014). Hence, it is necessary to optimize the concentration between the precursors and bioreductors to obtain nanosilver particles with the appropriate particle size.

Response surface methodology (RSM) models combined with experimental designs such as factorial design, central composite design (CCD), Box-Behnken design, and Doehlert design can be applied in natural product research (Riswanto *et al*., 2019). The CCD method is carried out to predict the optimal conditions and maximize the desired response as well as determine the relationship between variables and the dependent variable. In this study, the CCD method was applied since there is no need to spend much time and it is cheaper than the "one variable at a time" method that measures each influencing factor one by one (Yousefi *et al*., 2016). By applying the CCD, there is no need for a three-level factorial experiment to build an accurate predictive RSM model (Bhattacharya, 2021; Talluri *et al*., 2019). According to the description above, the optimal concentration of $AgNO_3$ and the bioreductor in the synthesis of nanosilver needs to be determined in order to achieve the desired response including appropriate wavelength and transmittance value. The aim of this research was to optimize the nanosilver formula consisting of the black tea leaf extract (*C. sinensis* L.) and $AgNO_3$ with the application of the CCD approach.

METHODS

Materials

The materials used in this research were black tea leaf simplicia (*C. sinensis* L.) from Lipton® Yellow Label Tea, redistilled water prepared (PT. Ikapharmindo Putramas), silver nitrate pro-analysis ($AgNO_3$), pharmaceutical-grade butanol, pharmaceutical-grade concentrated hydrochloric acid, pharmaceutical-grade acetic acid, and rutin standard (Merck) purchased from Merck Millipore.

Instruments

The tools used in this research are glassware (PT. Iwaki Glass), a thermometer, a magnetic stirrer, a UV-Vis spectrophotometer (Shimadzu UV-Vis 1800), a hot plate (Thermo Scientific), analytical balance (Ohaus), a TLC plate GF_{254} (Merck), a particle size analyzer (Horiba) equipped with Horiba SZ-100 for Windows ver. 2.00, a capillary tube, a vortex (Thermo Scientific), and a centrifuge (Thermo Scientific).

Nanosilver formula optimization design

According to the research by Zhou and Tang (2018), the approximate equation of the reaction for the formation of nanosilver is as follows:

$$2AgNO_3 + C_{27}H_{30}O_{16} \rightarrow 2Ag° + C_{27}H_{28}O_{16} + 2HNO_3 \quad \text{.....(1)}$$

Based on this reaction, it is necessary to optimize the concentration of $AgNO_3$ and the concentration of the black tea leaf extract to obtain the appropriate nanosilver formula. Table 1 presents the $AgNO_3$ concentration and extract concentration at each experimental level.

The optimization and data analysis were performed using the RSM approach, namely, CCD. The optimization in this research was assisted by the use of the Minitab 17 software. An experimental design with 16 runs was obtained for generating the optimization model.

The preparation of black leaf tea infusion (*C. sinensis* L.)

Black tea leaf powder (*C. sinensis* L.) was weighed to as much as 0.9751, 1.2298, 1.8448, 2.4596, and 2.7143 g, respectively. A 100 ml of redistilled water was heated to 90°C ± 2°C. Then, the tea leaf powder was put into the water and heated for 15 minutes at 90°C ± 2°C accompanied by the stirring process. The infusion obtained was filtered (Khafidhoh *et al*., 2015).

Table 1. Factors optimized using the CCD method.

Factors	Experimental levels for CCD				
	(−α)	(−1)	(0)	(+1)	(+α)
$AgNO_3$ concentration (mM)	0.80	1.00	1.50	2.00	2.20
Extract concentration (%m/v)	0.98	1.23	1.85	2.46	2.70

Thin-layer chromatography

The butanol-acetic acid-water phase with a ratio of 4: 1: 5 (v/v/v) was prepared by mixing the three ingredients, then shaking, and then letting it stand. The mobile phase would be formed into two layers. The top layer (butanol) was taken into the chromatography chamber, followed by a saturation process for 1 hour. The stationary phase used in this study was a silica gel GF_{254} thin-layer chromatography plate with a size of 5 × 10 cm and elution distance of 8 cm. The sample and rutin standard comparator were spotted. After the eluent was saturated, the chromatographic plate was put into the chamber and eluted with the mobile phase into the volume. The plate was observed under UV light with a wavelength of 254 and 365 nm. The Rf value was determined (Andersen and Maarkham, 2006; Aryantini *et al*., 2017; Sari and Meitisa, 2017).

Preparation of $AgNO_3$ solution

The solid $AgNO_3$ was dissolved using redistilled water. The solution was transferred into a 100 ml volumetric flask and diluted with redistilled water into the volume. The solution was shaken until it dissolved completely (Rengga *et al*., 2017).

Nanosilver synthesis and purification

Five milliliters of the black tea leaf (*C. sinensis* L.) infusion and 45 ml of the $AgNO_3$ solution were mixed in a beaker and stirred using a stirrer at the speed of 600 rpm for 10 minutes at ±75°C. This method was developed as a modification of the previous studies (Christania *et al*., 2020; Fabiani *et al*., 2019; Rengga *et al*., 2017; Zhou and Tang, 2018). Nanosilver purification was carried out by centrifuging colloid at the speed of 2,000 rpm for 15 minutes. The centrifuged supernatant was tested for wavelength, percent of transmittance, and the size of the particle (Dewi *et al*., 2019; Singh *et al*., 2016).

Nanosilver characterization

The nanosilver formed was analyzed using a UV-Vis spectrophotometer with a wavelength range of 400–450 nm (Sari *et al*., 2017). The measurement of the maximum wavelength used a UV-Vis spectrophotometer. The transmittance test was carried out using a UV-Vis spectrophotometer. A total of 100 µl of the nanosilver sample was dissolved in 5 ml of redistilled water and then was whirled into a vortex for 1 minutes. The sample was then measured for absorbance at the maximum wavelength. The blank used is redistilled water (Huda and Wahyuningsih, 2018).

Statistical analysis

The optimization process was carried out using the CCD method (two factors and five levels). The results of the study were analyzed by using the analysis of variance statistical test using the Minitab 17 software.

RESULTS AND DISCUSSION

Green synthesis of silver nanoparticles for antibacterial agents has attracted more interest in the field of pharmaceutical technology (Badnore *et al*., 2019; Sastry *et al*., 2019; Vishwasrao *et al*., 2019). This research aimed to optimize the nanosilver formula consisting of black tea leaf extract (*C. sinensis* L.) and $AgNO_3$ assisted by the CCD approach. The experimental design using CCD resulted in 16 experimental runs that varied the concentration of $AgNO_3$ and the concentration of the black tea leaf extract.

A qualitative test of flavonoids was carried out using the thin-layer chromatography method to verify the presence of rutin flavonoids in the infusion of black tea leaves. The qualitative test was carried out using the TLC test with rutin of 0.1% as the reference standard. The rutin standard showed the Rf value of 0.8125 while the *C. sinensis* extract was spotted at the Rf value of 0.8375. It was found that the black tea leaf extract contained rutin as it was proved by the closeness of the Rf value for both the reference standard and *C. sinensis* extract. The TLC results are presented in Figure 1.

At the initial stage, the mixture of the *C. sinensis* extract and $AgNO_3$ showed the color of light yellow. The color change from light yellow to reddish-brown indicated the formation of nanosilver. This result is related to the previous studies that reported the color change to brownish color occurred due to the presence of surface plasmon resonance and indicated the reduction process of silver ions (Dewi *et al*., 2019; Salem *et al*., 2018). After the nanosilver synthesis process was undertaken, purification was also carried out to remove the existing impurities. There was an increase in wavelength between before and after purification. Increasing the wavelength indicated that the size of the nanosilver particles which has been formed was getting bigger due to delocalization and exchange of conduction electrons on the surface of the particles which led to the occurrence of a bathochromic shift (Ahmad *et al*., 2018). A previous study reported that the agglomeration of nanosilver particles affected their size and altered the toxic response to *Moina macrocopa* (Borase *et al*., 2019).

According to a previous study, samples with wavelengths between 300 and 400 nm indicated that nanosilver had not yet

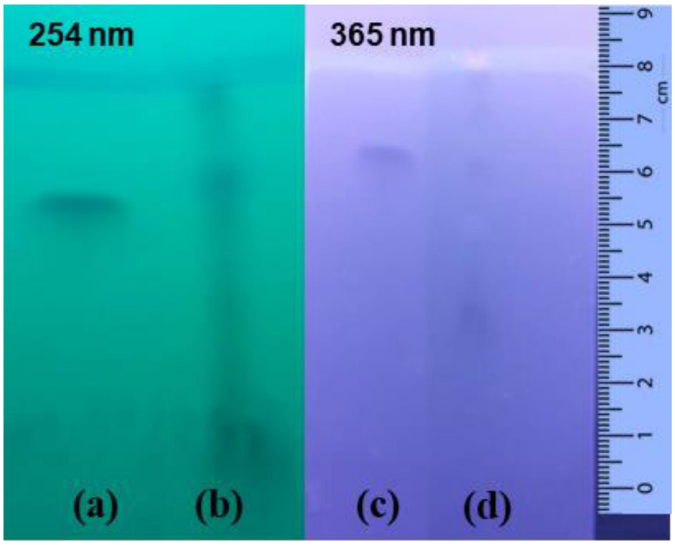

Figure 1. TLC results of rutin standard (a and c) and *C. sinensis* extract (b and d) at two different wavelengths' detection. Mobile phase: butanol-acetic acid-water with a ratio of 4:1:5 (v/v). Stationary phase: silica gel GF_{254}. The elution distance was 8 cm.

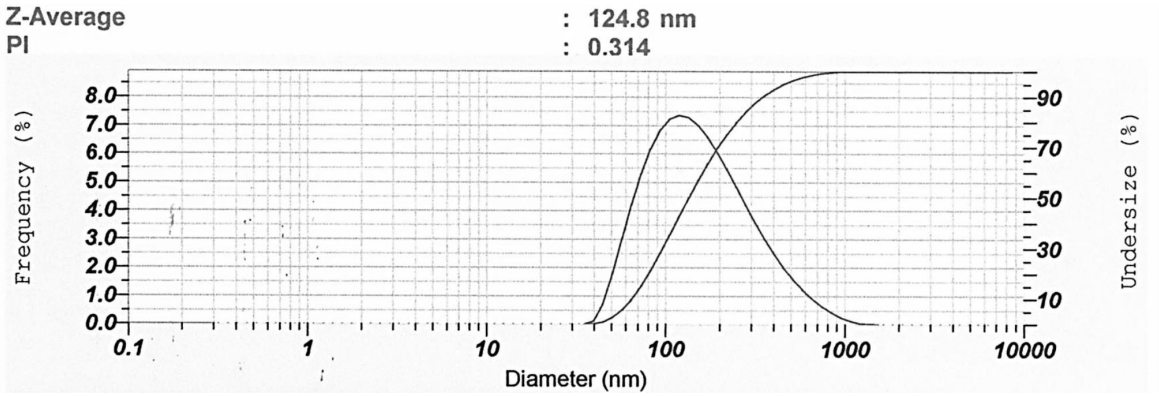

Figure 2. Representative of particle size analysis result of nanosilver particles.

Table 2. Experimental design with CCD approach and the response obtained from the observation.

Run order	Blocks	Independent variables		Dependent variables	
		$AgNO_3$ concentration (mM)	Extract concentration (% m/v)	Wavelength (nm)	Transmittance (%)
1	1	1.00	1.23	436.00 ± 5.29	88.90 ± 8.62
2	1	2.00	1.23	434.67 ± 5.77	83.90 ± 5.88
3	1	1.00	2.46	394.67 ± 82.20	81.97 ± 11.09
4	1	2.00	2.46	398.33 ± 82.59	72.47 ± 2.83
5	1	1.50	1.85	442.00 ± 11.69	83.60 ± 11.69
6	1	1.50	1.85	452.00 ± 11.69	85.30 ± 11.69
7	1	1.50	1.85	448.00 ± 11.69	85.50 ± 11.69
8	1	1.50	1.85	446.00 ± 11.69	86.70 ± 11.69
9	2	0.80	1.85	436.00 ± 4.00	89.50 ± 0.70
10	2	2.20	1.85	440.67 ± 10.26	84.20 ± 3.39
11	2	1.50	0.98	429.33 ± 8.33	90.70 ± 3.93
12	2	1.50	2.70	354.67 ± 97.00	78.90 ± 3.77
13	2	1.50	1.85	414.00 ± 11.69	85.70 ± 11.69
14	2	1.50	1.85	444.00 ± 11.69	86.80 ± 11.69
15	2	1.50	1.85	440.00 ± 11.69	88.60 ± 11.69
16	2	1.50	1.85	446.00 ± 11.69	86.60 ± 11.69

been formed (Ag^+) (Dewi *et al*., 2019). Hence, the expected wavelength in this study was in the range of 400–450 nm. Nugroho and Sari (2018) reported the percentage of transmittance above 70% already indicated the formation of nano-sized particles (< 200 nm). However, the percentage of transmittance that gets closer to 100% indicates that the sample is transparent and has nano-sized particles (Abdassah, 2009; Huda and Wahyuningsih, 2018). The blank used for nanoparticle characterization was redistilled water. In this study, water was selected as the solvent since it was suitable for specified reactions and is reported to be successfully applied in nanoparticle synthesis (Muley *et al*., 2020). The resulting nanosilver particles were characterized and presented in Figure 2. The Z-average represents the grand average of all of the intensities measured by dynamic light scattering. In nanoparticle formulation, a polydispersity index of 0.3 and below is considered to be acceptable (Danaei *et al*., 2018). However, the PI of lower than 0.5 indicating a narrow and favorable particle size distribution (Mohammadpour Dounighi *et al*., 2012).

Table 2 presents the experimental design using the CCD approach and the responses obtained including wavelength and transmittance percentage. Regression analysis using RSM was performed with Minitab 17. Table 3 shows the results of the response surface regression analysis for wavelength and transmittance percentage.

The response surface model for the wavelength showed significant results in terms of $p < 0.05$. The p-value for lack-of-fit shows a value above 0.05 indicating that the discrepancy generated by the model was not significant. The regression equation for the wavelength model was as follows: wavelength = 284.5 + 11.5 AC + 196.3 EC − 5.6 AC × AC − 64.96 EC × EC + 4.1 AC × EC (AC: $AgNO_3$ concentration; EC: *C. sinensis* extract concentration). The values of R^2 and R^2 (adj) were obtained to be greater than 80% with a difference of more than 2%. Hence, it can be stated

Table 3. Results of response surface regression analysis for wavelength and transmittance percentage.

Source	Wavelength					Percentage of transmittance				
	DF	Adj SS	Adj MS	*F*-value	*p* value	DF	Adj SS	Adj MS	*F*-value	*p* value
Model	6	9194.5	1532.41	14.98	0.000	6	276.305	46.051	19.37	0.000
Blocks	1	138.1	138.06	1.35	0.275	1	32.111	32.111	13.50	0.005
Linear	2	4208.1	2104.03	20.56	0.000	2	214.075	107.037	45.01	0.000
$AgNO_3$	1	10.0	9.97	0.10	0.762	1	60.474	60.474	25.43	0.001
Ekstrak	1	4198.1	4198.08	41.03	0.000	1	153.601	153.601	64.59	0.000
Square	2	4842.1	2421.06	23.66	0.000	2	25.057	12.528	5.27	0.031
$AgNO_3 \times AgNO_3$	1	15.6	15.59	0.15	0.705	1	3.167	3.167	1.33	0.278
Extract × extract	1	4826.5	4826.53	47.17	0.000	1	21.89	21.89	9.21	0.014
2-way interaction	1	6.2	6.25	0.06	0.810	1	5.062	5.062	2.13	0.179
$AgNO_3$ × extract	1	6.2	6.25	0.06	0.810	1	5.062	5.062	2.13	0.179
Error	9	920.8	102.31			9	21.402	2.378		
Lack-of-fit	3	204.8	68.28	0.57	0.654	3	12.087	4.029	2.60	0.148
Pure error	6	716	119.33			6	9.315	1.553		
Total	15	10115.3				15	297.707			
Model summary	S = 10.1151; R^2 = 90.90%; R^2(adj) = 84.83%; R^2(pred) = 73.07%					S = 1.54206; R^2 = 92.81%; R^2(adj) = 88.02%; R^2(pred) = 61.89%				

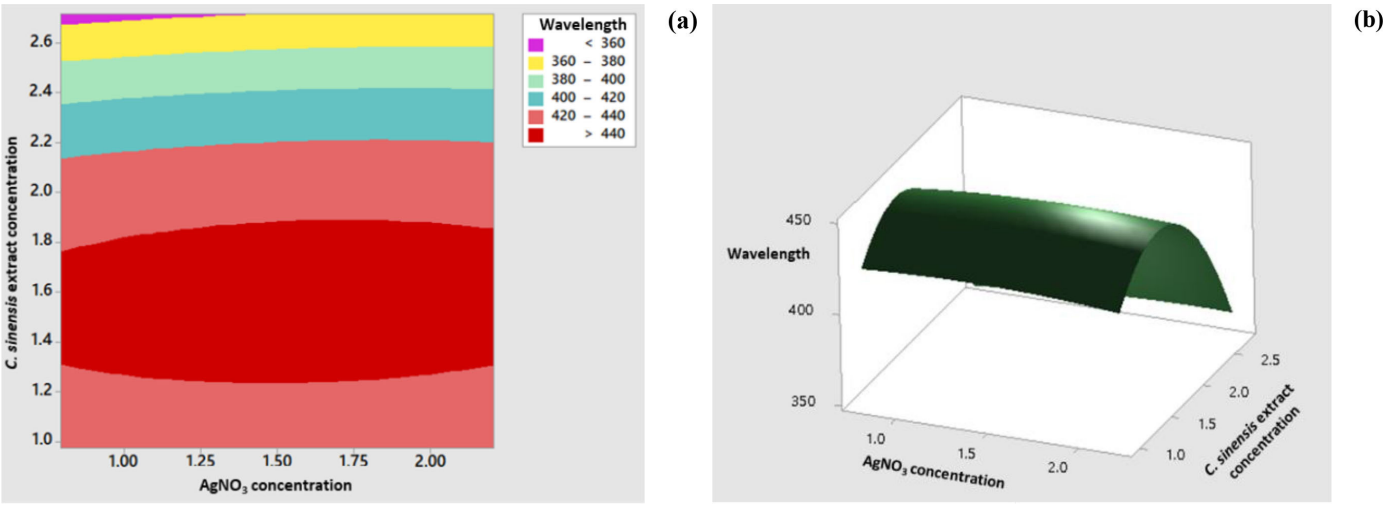

Figure 3. Contour plot (a) and surface plot (b) of the wavelength versus concentration of *C. sinensis* extract and $AgNO_3$.

that the model built can be employed to predict the wavelength significantly. Figure 3 shows the appearance of the contour plot and surface plot of wavelength versus extract concentration and transmittance percentage.

The response surface model for the percentage of transmittance showed significant results in terms of $p < 0.05$. The p value for lack-of-fit shows a value above 0.05 indicating that the discrepancy generated by the model was not significant. The regression equation for the percentage transmittance model was as follows: %transmittance = 76.82 + 8.80 AC + 14.50 EC − 2.52 AC × AC − 4.37 EC × EC − 3.66 AC × EC (AC: $AgNO_3$ concentration; EC: *C. sinensis* extract concentration). The values of R^2 and R^2 (adj) were obtained to be greater than 80% with the difference of more than 2%. Hence, it can be stated that the model built can be employed to predict the wavelength significantly. The appearance of the contour plot and surface plot of transmittance percentage versus extract concentration and transmittance percentage are depicted in Figure 4.

The process of determining the optimum formula was carried out using the response optimizer menu since it was reported in a previous study that the multiple response optimization can be carried out using the Minitab software (Dwiastuti *et al.*, 2021). The optimization target was set up with a target wavelength at 425 nm (the lower limit was at 400 nm, and the upper limit was at 450 nm), and the percentage of transmittance was at maximum conditions. The extract concentration of 2.131% (m/v) and the $AgNO_3$ concentration of 1.379 mM were found as the computational recommendation to achieve the optimum condition. These concentrations were predicted to produce a composite desirability value of 0.998. A desirability value close to 1 indicates a high model's ability to produce the expected value. Figure 5

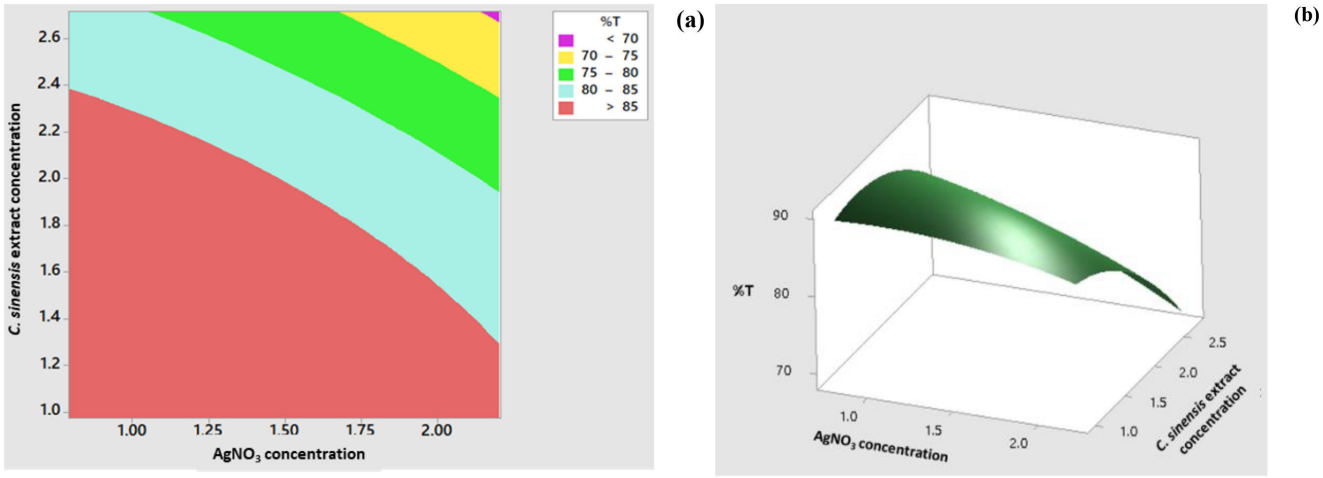

Figure 4. Contour plot (a) and surface plot (b) percentage of transmittance versus concentration of *C. sinensis* extract and $AgNO_3$.

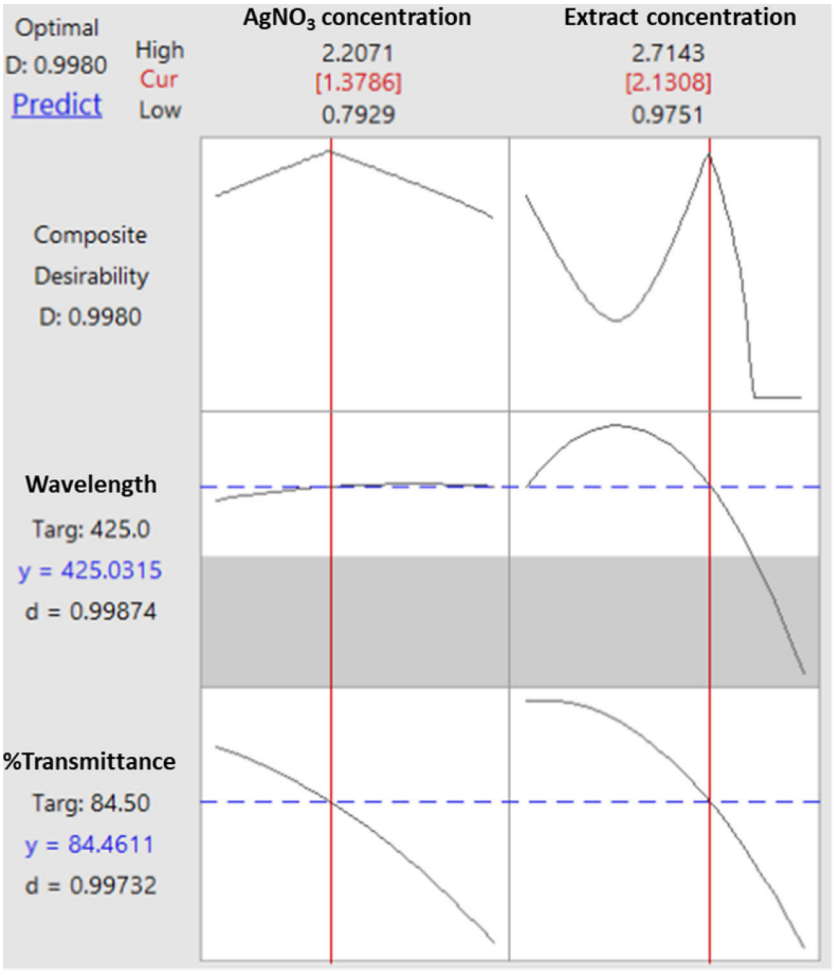

Figure 5. Optimization plot for wavelength and transmittance percentage.

shows optimization plots for both responses including wavelength and transmittance percentage.

The optimum formula obtained from the RSM model was formulated in the production of nanosilver. The results were obtained from the observation of six replications of the formula as shown in Table 4. The visible absorption wavelength was 444.33 ± 12.49 nm, whereas the percentage of transmittance was 80.65% ± 1.78%. Figure 6 presents representative visible spectra of the nanosilver formula with low transmittance (high absorbance), medium transmittance (medium absorbance), and high transmittance (low absorbance). It can be observed that the percentages of the prediction relative error (REP) of the

Table 4. Results of optimum formula testing on wavelength response and transmittance percentage.

No	Wavelength (nm)	REP wavelength (%)	Transmittance (%)	REP transmittance (%)
1	452	6.35	81.40	3.67
2	430	1.18	80.50	4.73
3	464	9.18	77.20	8.64
4	440	3.53	82.20	2.72
5	446	4.94	81.60	3.43
6	434	2.12	81.00	4.14
Mean	444.33		80.65	
SD	12.49		1.78	
RSD (%)	2.81		2.21	

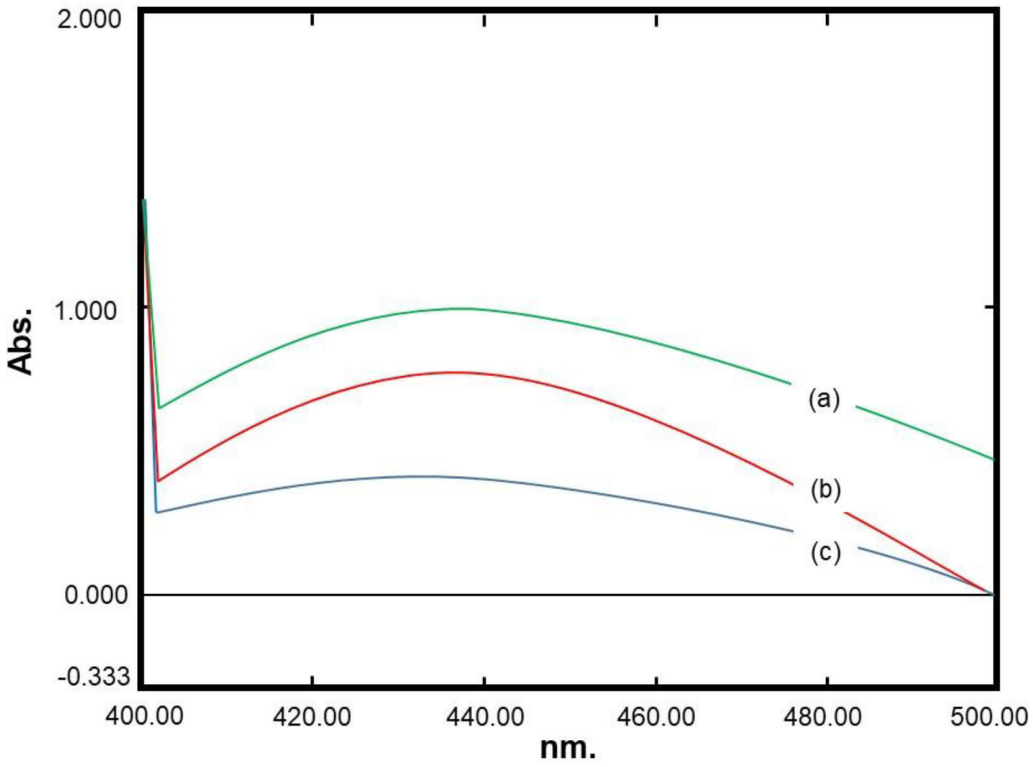

Figure 6. Representative visible spectra of nanosilver formula with low transmittance (a), medium transmittance (b), and high transmittance (c).

wavelength and transmittance are in the ranges of 1.18%–9.18% and 2.72%–8.64%, respectively. The RSD values which indicate that there were random errors in determining the observation results for the wave and transmittance were 2.81% and 2.21%, respectively. These results indicated that the optimum formula obtained from the RSM model for nanosilver particles had been achieved. However, it is recommended that further comprehensive studies on degradation, antibacterial activity, and cytotoxicity as well as the enzymatic observation are carried out in the future to elaborate on the research regarding the development of nanosilver particle synthesis (Momin *et al*., 2019; Muley *et al*., 2020).

CONCLUSION

The optimum formula for the extract concentration of *C. sinensis* L. leaf and the concentration of $AgNO_3$ in the nanosilver formulation was obtained using the CCD approach. Optimum conditions achieved in this study were *C. sinensis* extract concentration of 2.131% (w/v) and $AgNO_3$ concentration of 1.379 mM. This condition resulted in a composite desirability value of 0.998 in the computational optimization process. The results of formula observation under the optimum conditions produced good repeatability with a minimum prediction error of less than 10% for both the wavelength response and transmittance percentage.

ACKNOWLEDGMENT

The authors would like to thank Michael Raharja Gani (Universitas Sanata Dharma, Yogyakarta, Indonesia) for assistance with the spectroscopic measurement.

CONFLICT OF INTEREST

All the authors declared there are no conflicts of interest.

AUTHOR CONTRIBUTIONS

Rini Dwiastuti and Phingkan Alamanda Suhendra carried out the optimization research, data investigation, and initial draft writing. Sri Hartati Yuliani reviewed the initial draft and supervised the content in the field of natural product research and optimization techniques. Florentinus Dika Octa Riswanto provided the conceptualization of the article and supervised the content in the field of analytical chemistry and RSM.

FUNDING

This research was financially funded by Program Penelitian Pusat Studi Universitas Sanata Dharma 2021 (No.:13/ Penel./LPPM-USD/II/2021) awarded to Dr. apt. Rini Dwiastuti, M.Sc.

ETHICAL APPROVALS

This study does not involve experiments on animals or human subjects.

DATA AVAILABILITY

All data generated and analyzed are included within this research article.

PUBLISHER'S NOTE

This journal remains neutral with regard to jurisdictional claims in published institutional affiliation.

REFERENCES

Abdassah M. Nanopartikel dengan gelasi ionik. Farmaka, 2009; 15(1):45–52.

Andersen ØM, Markham KR. Flavonoids: chemistri, biochemistry, and applications. Taylor & Francis Group, London, UK, 2006.

Ahmad N, Ang BC, Amalina MA, Bong CW. Influence of precursor concentration and temperature on the formation of nanosilver in chemical reduction method. Sains Malaysiana, 2018; 47(1):157–68.

Aizawa Y, Sunada S, Hirakawa H, Fujimori A, Kato TA, Uesaka M. Design and evaluation of a novel flavonoid-based radioprotective agent utilizing monoglucosyl rutin. J Radiat Res, 2018; 59(3):272–81.

Anesini C, Ferraro GE, Filip R. Total polyphenol content and antioxidant capacity of commercially available tea (*Camellia sinensis*) in Argentina. J Agric Food Chem, 2008; 56(19):9225–9.

Aryantini D, Sari F, Juleha J. Uji aktivitas antibakteri fraksi aktif terstandar flavonoid dari daun belimbing wuluh (*Averrhoa bilimbi* L.). J Wiyata, 2017; 4(2):143–50.

Badnore AU, Sorde KI, Datir KA, Ananthanarayan L, Pratap AP, Pandit AB. Preparation of antibacterial peel-off facial mask formulation incorporating biosynthesized silver nanoparticles. Appl Nanosci, 2018; 9(2):279–87.

Bhattacharya S. Central Composite Design for Response Surface Methodology and Its Application in Pharmacy. In: Response Surface Methodology in Engineering Science, London: IntechOpen, 2021. p. 1–20.

Borase HP, Patil SV, Singhal RS. *Moina macrocopa* as a non-target aquatic organism for assessment of ecotoxicity of silver nanoparticles: effect of size. Chemosphere, Pergamon, 2019; 219:713–23.

Christania FS, Dwiastuti R, Yuliani SH. Lipid and silver nanoparticles gels formulation of tempeh extract. J Pharm Sci Community, 2020; 16(2):56–62.

Danaei M, Dehghankhold M, Ataei S, Hasanzadeh Davarani F, Javanmard R, Dokhani A, Khorasani S, Mozafari MR. Impact of particle size and polydispersity index on the clinical applications of lipidic nanocarrier systems. Pharmaceutics, 2018; 10(2):1–17.

Demchenko V, Riabov S, Sinelnikov S, Radchenko O, Kobylinskyi S, Rybalchenko N. Novel approach to synthesis of ssilver nanoparticles in interpolyelectrolyte complexes based on pectin, chitosan, starch and their derivatives complexes based on pectin , chitosan , starch and their derivatives. Carbohydr Polym, 2020; 242:116431.

Deshmukh SP, Patil SM, Mullani SB, Delekar SD. Silver nanoparticles as an effective disinfectant : a review. Mater Sci Eng C, 2019; 97:954–65.

Dewi KTA, Kartini K, Sukweenadhi J, Avanti C. Karakter fisik dan aktivitas antibakteri nanopartikel perak hasil green synthesis menggunakan ekstrak air daun sendok (*Plantago major* L.). JPSR, 2019; 6(2):69–81.

Dong Y, Zhu H, Id YS, Zhang W, Zhang L. Antibacterial activity of silver nanoparticles of different particle size against vibrio natriegens. PLoS One, 2019; 14(9):1–12.

Dwiastuti R, Putri DCA, Hariono M, Riswanto FDO, Short communication: multiple response optimization of an HPLC method for analyzing resorcinol and 4-n-butyl resorcinol in lipid nanoparticles. Indones J Chem, 2021; 21(2):502–11.

Enogieru AB, Haylett W, Hiss DC, Bardien S, Ekpo OE. Rutin as a potent antioxidant: implications for neurodegenerative disorders. Oxid, 2018; 2018:6241017.

Fabiani VA, Putri MA, Saputra ME, Indriyani DP. Sintesis nanosilver menggunakan bioreduktor ekstrak daun pelawan (*Tristaniopis merguensis*) dan uji aktivitas antibakteri. J Kim dan Pendidik Kim, 2019; 4(3):172–8.

Ge LP, Li QT, Wang M, Jun OY, Li XJ, Xing MM. Nanosilver particles in medical applications : synthesis, performance, and toxicity. Int J Nanomedicine, 2014; 9:2399–407.

Handayani W, Ningrum AS, Imawan C. The eole of pH in synthesis silver nanoparticles using *Pometia pinnata* (Matoa) leaves extract as bioreductor. J Phys Conf Ser, 2020; 1428(1):1–5.

Huda N, Wahyuningsih I. Karakterisasi self-nanoemulsifying drug delivery system (SNEDDS) minyak buah merah (*Pandanus conoideus* Lam.). JFKI, 2018; 3(2):49.

Jiang H, Engelhardt UH, Thrane C, Maiwald B, Stark J. Antibacterial mechanism of silver nanoparticles in: *Pseudomonas aeruginosa*: proteomics approach. Metallom, Royal Soc Chem, 2015; 10(4):557–64.

Khafidhoh Z, Dewi SS, Iswara A. Efektivitas infusa kulit jeruk purut (Citrus hystrix DC.) terhadap pertumbuhan Candida albicans. The 2nd University Research Colloquium, Semarang: LPPM Universitas Muhammadiyah Semarang, 2015. p. 31–37.

Khalil MMH, Ismail EH, El-Baghdady KZ, Mohamed D. Green synthesis of silver nanoparticles using olive leaf extract and its antibacterial activity. Arab J Chem, King Saud Univ, 2014; 7(6):1131–9.

Kupiec A, Malina D, Wzorek Z, Zimowska M. Influence of silver nitrate concentration on the properties of silver nanoparticles. Micro Nano Lett, 2011; 6(8):656–60.

Latos-Brozio M, Masek A. Structure-activity relationships analysis of monomeric and polymeric polyphenols (quercetin, rutin and catechin) obtained by various polymerization methods. Chem Biodivers, 2019; 16(12):1–14.

Li X, Xu H, Chen ZS, Chen G. Biosynthesis of nanoparticles by microorganisms and their applications. J Nanomater, 2011; 2011:1–16.

Maarebia RZ, Wahid Wahab A, Taba P. Synthesis and characterization of silver nanoparticles using water extract of sarang semut (*Myrmecodia pendans*) for blood glucose sensors. Akta Kim Indones, 2019; 12(1):29.

Mohammadpour Dounighi N, Damavandi M, Zolfagharian H, Moradi S. Preparing and characterizing chitosan nanoparticles containing

hemiscorpius lepturus scorpion venom as an antigen delivery system. Arch Razi Inst, 2012; 67(2):145–53.

Momin B, Rahman S, Jha N, Annapure US. Valorization of mutant *Bacillus licheniformis* M09 supernatant for green synthesis of silver nanoparticles: photocatalytic dye degradation, antibacterial activity, and cytotoxicity. Bioprocess Biosyst Eng, 2019; 42(4):541–53.

Muley AB, Mulchandani KH, Singhal RS. Immobilization of enzymes on iron oxide magnetic nanoparticles: synthesis, characterization, kinetics and thermodynamics. Methods Enzymol, 2020; 630:39–79.

Nugroho BH, Sari NP. Formulation of self nano emulsifiying drug delivery system (SNEDDS) karamunting leaf extract (*Rhodomyrtus tomentosa* (Ait.) Hassk). J Ilm Farm, 2018; 14(1):1–8.

PubChem. Rutin, 2020. Available via https://pubchem.ncbi.nlm.nih.gov/compound/Rutin (Accessed 29 March 2020).

Pulit J, Banach M, Kowalski Z. Chemical reduction as the main method for obtaining nanosilver chemical reduction as the main method for obtaining nanosilver. J Comput Theor Nanosci, 2015; 10(2):1–9.

Ravindra S, Mohan YM, Reddy NN, Raju KM. Colloids and surfaces A : physicochemical and engineering aspects fabrication of antibacterial cotton fibres loaded with silver nanoparticles via "Green Approach." Coll Surf A, 2010; 367:31–40.

Rengga WDP, Yufitasari A, Adi W. Synthesis of silver nanoparticles from silver nitrate solution using green tea extract (*Camelia sinensis*) as bioreductor. JBAT, 2017; 6(1):32–8.

Riswanto FDO, Rohman A, Pramono S, Martono S. Application of response surface methodology as mathematical and statistical tools in natural product research. J Appl Pharm Sci, 2019; 9(10):125–33.

Salem H, Elhela AA, Abdelhady NM. Utility of silver nanoparticles for the analysis of diosmin and rutin in *Persicaria salicifolia* extract, authentic and pharmaceutical dosage forms monitored with their haemostatic activity. African J Pharm Pharmacol, 2018; 12(20):248–62.

Sankar KPC, Ramakrishnan R, Rosemary MJ. Biological evaluation of nanosilver incorporated cellulose pulp for hygiene products. Mater Sci Eng C, 2016; 61:631–7.

Sari ER, Meitisa M. Standarisasi mutu ekstrak daun singkong (*Manihot esculenta* Crantz). J Ilm Bakti Farm, 2017; 2(1):13–20.

Sari PI, Firdaus ML, Rina E. Pembuatan nanopartikel perak (NPP) dengan bioreduktor ekstrak buah *Muntingia calabura* L untuk analisis logam merkuri. Alotrop, 2017; 1(1):20–6.

Sastry SKC, Jadhav NL, Doltade SB, Pinjari DV. Effect of concentrated solar radiation on the morphology of the silver nanoparticles and its antibacterial activity. Indian Chem Eng, 2019; 61(4):374–86.

Singh P, Kim YJ, Wang C, Mathiyalagan R, El-Agamy Farh M, Yang DC. Biogenic silver and gold nanoparticles synthesized using red ginseng root extract, and their applications. Artif Cells Nanomed Biotechnol, 2016; 44(3):811–6.

Talluri VP, Lanka SS, Saladi VR. Statistical optimization of process parameters by Central Composite Design (CCD) for an enhanced production of L-asparaginase by Myroides gitamensis BSH-3, a novel species. Avicenna J Med Biotechnol, 2019; 11(7):59–66.

Tariq M, Naveed A, Barkat AK. The morphology, characteristics, and medicinal properties of *Camellia sinensis* Tea. J Med Plant Res, 2010; 4(19):2028–33.

Tong T, Liu YJ, Kang J, Zhang CM, Kang SG. Antioxidant activity and main chemical components of a novel fermented tea. Molecules, 2019; 24(16):1–14.

Turkmen N, Veliogla YS, Sari F, Polat G. Effect of extraction conditions on measured total polyphenol contents and antioxidant and antibacterial activities of black tea. Molecules, 2007; 12(3):484–96.

Vishwasrao C, Momin B, Ananthanarayan L. green synthesis of silver nanoparticles using sapota fruit waste and evaluation of their antimicrobial activity. Waste Biomass Valoriz, 2018; 10(8):2353–63.

Wendri N, Rupiasih NN, Sumadiyasa M. Biosintesis nanopartikel perak menggunakan ekstrak daun sambiloto: optimasi proses dan karakterisasi. JUSAMI, 2017; 18(4):162.

Yousefi N, Pazouki M, Hesari A, Alizadeh M. Statistical evaluation of the pertinent parameters in biosynthesis of Ag / MWf-CNT composites using plackett-burman design and response surface methodology. Iran J Chem Chem Eng, 2016; 35(2):51–62.

Zhou Y, Tang RC. Facile and eco-friendly fabrication of colored and bioactive silk materials using silver nanoparticles synthesized by two flavonoids. Polymers (Basel), 2018; 10(4):404.

How to cite this article:
Dwiastuti R, Suhendra PA, Yuliani SH, Riswanto FDO. Application of the central composite design approach for optimization of the nanosilver formula using a natural bioreductor from *Camellia sinensis* L. extract. J Appl Pharm Sci, 2022; 12(08):048–056.